SAE AERODESIGN WEST

"THE WRIGHT STUFF"

By
AARON LOSTUTTER, ADAM NELESSEN, JACOB VINCENT, ZEV VALLANCE, AND BRANDON PEREZ
Team 10

ENGINEERING ANALYSIS

Document

Submitted towards partial fulfillment of the requirements for
Mechanical Engineering Design – Fall 2012

Department of Mechanical Engineering
Northern Arizona University
Flagstaff, AZ 86011

Table of Contents

List of Tables and Figures

1. Introduction

The following report discusses the engineering analysis and all ensuing assumptions for the SAE AeroDesign West team "The Wright Stuff". The report will cover static analysis, theoretical design with emphasis on aerodynamics, propulsion systems, and lastly, spar analysis. Matlab codes and detailed calculations can be found in Appendix A and Appendix B at the end of this report.

2. Static Analysis

An important initial step of designing an aircraft is ensuring static equilibrium of the body during level flight. To meet this condition, the weight of the plane must be balanced by the lift generated by the airfoils and the resulting drag must be overcome by thrust. This can be accomplished through adequate balance of the lift produced by the wings in relation to the lift due to the tail. In addition, the moments about the center of gravity of the plane must also sum to zero to maintain static equilibrium. Placing the tail accordingly will ensure this balance of moments. By defining a term called the Lift Ratio as the lift from the wings divided by the lift from the tail and conducting the static analysis, the result is a system of equations relating these parameters in a way that guarantees level flight. The resulting equations and a figure used to derive these equations are shown below in **Figure 1** and **Equations 1, 2, and 3**.

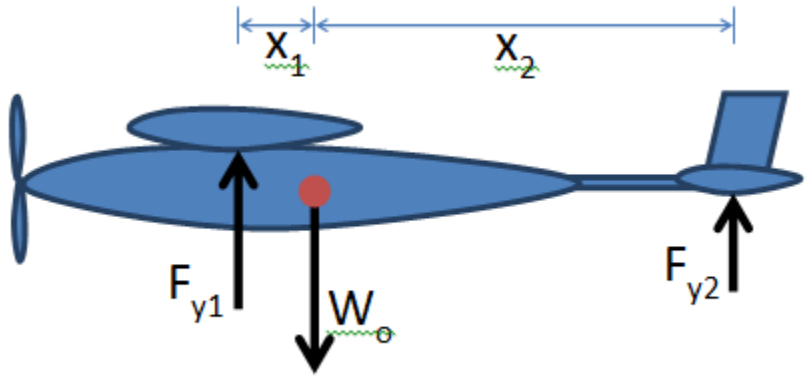

Figure 1: Static Analysis

$$x_2 = LR \times x_1 \tag{1}$$

$$F_{y1} = \frac{LR}{LR+1} \times W_o \tag{2}$$

$$F_{y2} = \frac{1}{LR+1} \times W_o \tag{3}$$

3. Aerodynamic Systems

In designing an aircraft, it is crucial to know the environmental characteristics such as air density, temperature, and aircraft velocity. Using historic values from our competition location and estimated velocities of the aircraft, we determine a Reynolds number range between 282,000 and 450,000. Knowing that our aircraft will be operating below a Reynolds number of 500,000 is important because it lays out the fundamental characteristic for the type of aircraft we will have; Reynolds numbers below 500,000 represents laminar flow. Flying in laminar flow determines the types of drag that are crucial. For these parameters, pressure drag will be significantly more than the skin friction. This is highly important in determining the type of airfoil the aircraft will be utilizing. In addition, induced drag will play a significant role in the competition, where determining the type of planform geometry is vital. Another key characteristic is the Mach number. For any Mach number below 0.3, the flow is assumed to be incompressible. Our Mach number is calculated to be about 0.053, much below 0.3, therefore, aerodynamically, our aircraft will be designed to fly in laminar and incompressible flow

3.1. Airfoil selection

Once the flow characteristics were defined, it was found that in determining the type of airfoil, a high lift and minimal drag type of airfoil will be needed; because the pressure drag is most significant, an airfoil with minimal pressure drag will be needed while simultaneously providing the high lift characteristics of a cambered airfoil. This is imperative because the type of airfoil will have to reduce the flow separation (minimize the boundary layer) while still having the lift characteristics of a high cambered airfoils that that produced large coefficients of lift in addition to having minimal pressure drag. There are many options for airfoils to choose from that have already been designed by NACA, Eppler and Selig for low Reynolds numbers and incompressible flow characteristics. Some airfoil considerations include:

- NACA 2408
- NACA 2412
- E174
- E180
- S1223

In addition, the aircrafts planform geometry will be designed to minimize the lift induced drag. Lift induced drag is produced by the wing tip vortices (high and low pressure above and below the wings) causing drag to increase and also reducing the effective angle of attack for the wings. Lift induced drag is defined by the following equation:

$$C_{D,i} = \frac{{C_L}^2}{\pi\, AR}(1 + \delta) \tag{4}$$

Equation 4 shows that the lift induced drag is highly a function of the aspect and taper ratios for the wing design. Aspect ratio is defined by **Equation 5** below:

$$AR = \frac{b^2}{S} \tag{5}$$

Where "b" is the wingspan of the wings and "S" is the planform area. For example, if there was a very large wingspan with very short chord length, the aspect ratio is increased. Having a large aspect ratio results in very minimal lift induced drag.

Figure 2 below displays the calculations for determining delta in finding the lift induced drag. For a give taper and aspect ratio, delta can be found and inserted into Equation 1. The taper ratio is defined by the chord at the tip of the wing divided by the chord at the root of the wing.

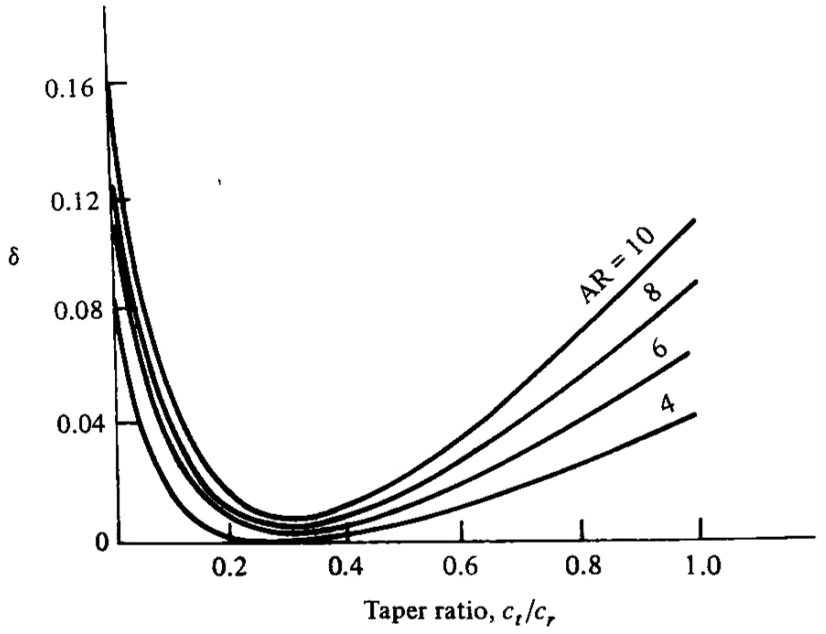

Figure 2: Drag coefficients as a function of the taper ratio and aspect ratio

Figure 2 really demonstrates the importance of using the optimal taper ratio, for instance, using a taper ration of 0.3 will result in the minimal delta (δ).

Using **Equation 4** and **Figure 2**, **Figure 3** displays an optimization surface plot from Matlab for an array of taper and aspect ratios. This allows the team to design the wings with minimal induced drag.

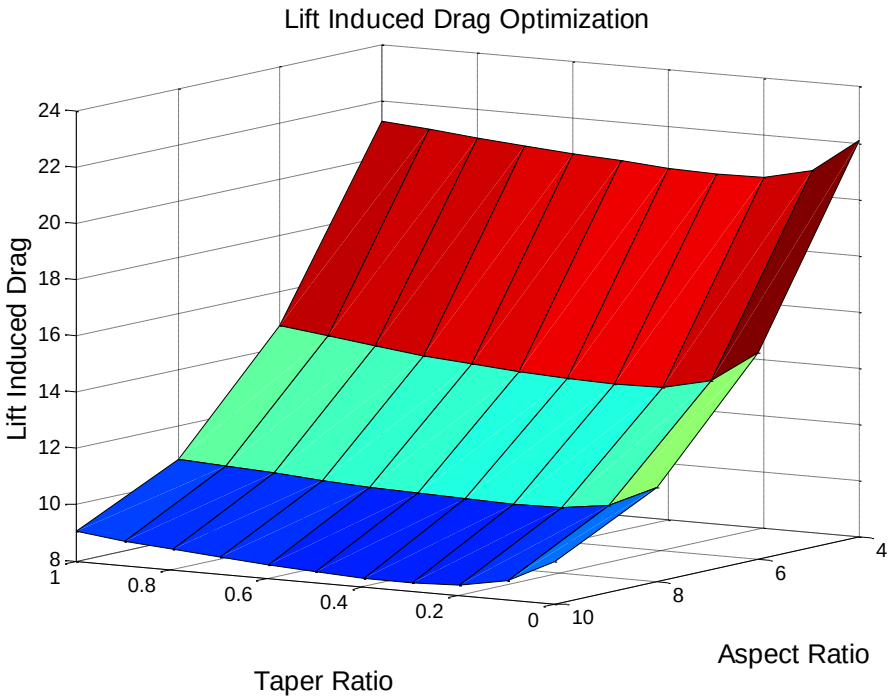

Figure 3: Lift induced drag optimization surface plot

Figure 3 demonstrates that for a taper ratio of about 0.3 and maximum aspect ratio of about ten, the optimal lift induced drag is achieved.

3.2. Theory of Wing Design

Once the airfoil is determined, it can be subject to multiple software programs for analysis. The first program was made in Matlab in a previous semester's aerodynamics class with Dr. Tom Acker. This method of analysis is called the vortex panel method where the airfoil geometry is discretized into a number of panels defining its cross-sectional shape. By inputing the airfoil geometry, chord length, angle of attack and some environmental conditions such as air density and the velocity of the aircraft, the vortex at each panel can be calculated and the program will output the lift and pressure coefficients per unit span. The program can also generate the coefficients for a sequence of angles of attack which will be useful in determining the optimal lift and drag angles for the airfoil.

The second piece of software is called XFOIL and "it is an interactive program for the design and analysis of subsonic isolated airfoils" [6]. It was first designed by a Professor at MIT, Mark Drela and then advanced with Harold Youngren. This program is very similar to the Matlab script that the team has developed however XFOIL provides many more opportunities. Not only does it produce the coefficient of lift and pressure, it also provides the drag coefficient as a function of pressure and viscous forces for a multiplicity of angles of attack.

Using the output from these two programs allows the design of the wings to be defined and optimized. This process was performed using the Matlab script as shown in Appendix A.

By defining the dynamic pressure of the system, q_{inf}, as shown in **Equation 6,** it can be employed with the lift coefficient produced from the programs developed from the S1223 airfoil, **Equation 7** calculates the the "prime" lift for a given chord length. The airfoil chord has been defined as 1 ft (0.3048 m).

$$q_{inf} = \frac{1}{2} * \rho * V^2 \tag{6}$$

$$L' = cl * q_{inf} * C \tag{7}$$

For a predetermined value of lift that we have defined as 80 Ib (355.8 N) to be able to provide enough lift for a maximum aircraft weight of 65 Ib (289.1 N) as required by the SAE AERO Design West Competition, is labeled as L_{square} below in **Equation 8**.

$$b = \frac{L_{Square}}{L'} \tag{8}$$

Using **Equation 8**, the wingspan, b, is determined for the aircraft to provide the lift necessary for the payload goal in the competition.

Given that the necessary lift from a square planform, the wing designed is tapered to reduce the lift induced drag as described above and as shown in **Figure 3**. This requires the integration of the lift about the length of the wing for the tapered planform in order to calculate the fractional lift of the wing as defined by the following equations:

$$L_{fraction} = 1 - \frac{(b*(C-C_{Tip}))}{(2*b*C)} \tag{9}$$

$$L_{Tapered} = L_{fraction} * L_{Square} \tag{10}$$

Now that the wings are defined by the previous analysis, the lift has been calculated using **Equation 9**. The planform area, S, can now also be calculated by simply calculating the area of the rectangular portion of the wing in addition to the triangular sections as defined by **Equation 11** below.

$$S = b * C_{Tip} + \left(C - C_{Tip}\right) * \left(\frac{b}{2}\right) \tag{11}$$

Now the primary lift coefficient, C_L, can be calculated as defined by the following equation:

$$C_L = \frac{L_{Tapered}}{q_{inf}*S} \tag{12}$$

The validity of the results will be tested by performing wind tunnel experiments for the aircrafts wing design. The wind tunnel experiment will be measured for similar Reynolds numbers to calculate both the lift and drag forces for the designed wing and these results will be compared to the theoretical solutions from the computer programs.

3.3. Methodology for Wing Design

The method employed for aerodynamic analysis relies on the use of XFOIL software, a Matlab code written by the team, and wind tunnel testing for validation purposes. XFOIL, a free two-dimensional software program that relies on the vortex lattice method, determines the performance characteristics of an airfoil per chord and wingspan. The Matlab program then accepts these characteristics from XFOIL simulations as well as environmental conditions and geometry estimates. Subsequently, this program computes the resulting wing shape and dimensions and determines the actual lift and drag produced by utilizing the theory described above in Section 2.2. These results are output into the command window of Matlab in an output table. The .m file used in this analysis is attached in Appendix A of this document.

i. Input airfoil geometry into XFOIL bin folder in .data format
ii. Input Reynolds number, Mach number, and a range of angles of attack into XFOIL
iii. Record XFOIL outputs of cl, cd, and cm occurring at the optimal angle of attack where cl/cd is a maximum
iv. Input into Matlab code the desired chord length at the wing root [ft], desired taper ratio, cl and cd from xfoil, and delta from Figure 1
v. Tabulate important outputs from Matlab code, such as: chord at the wing tip (ctip), wingspan (b), wing planform (S), aspect ratio (AR), lift generated by tapered wings (Ltapered), coefficient of induced drag (cDinduced), coefficient of 3D skin friction and pressure drag (cD_3D), overall coefficient of drag (CDtotal), and resulting drag (D)
vi. Repeat steps 1-5 for a variety of airfoil shapes, operating conditions, and wing geometries until the optimal shape is determined
vii. Validate numerical simulations with wind tunnel tests in which a scale model of the wing with accurate taper and airfoil cross section is tested for lift, drag, and moment production

3.4. Preliminary Results of Aerodynamic Analysis:

After a bit of research on airfoil types, the team decided to pursue the S1223 airfoil for the first iteration of this analytical procedure, because of its known ability to operate well in heavy-lift applications in low Reynolds numbers.

After conducting steps 1-3 of the analysis laid out in section 2.3 using the S1223 airfoil geometry, performance characteristics such as cl, cd, and cm were computed for various angles of attack. The outputs from XFOIL displaying this relevant data can be seen in **Figure 4** on following page. From inspection of this graphic, the maximum cl/cd occurs at an angle of attack of 12 degrees. Then, a simulation is performed to demonstrate the detailed performance of this airfoil at 12 degrees; the result is shown in **Figure 5** on the following page.

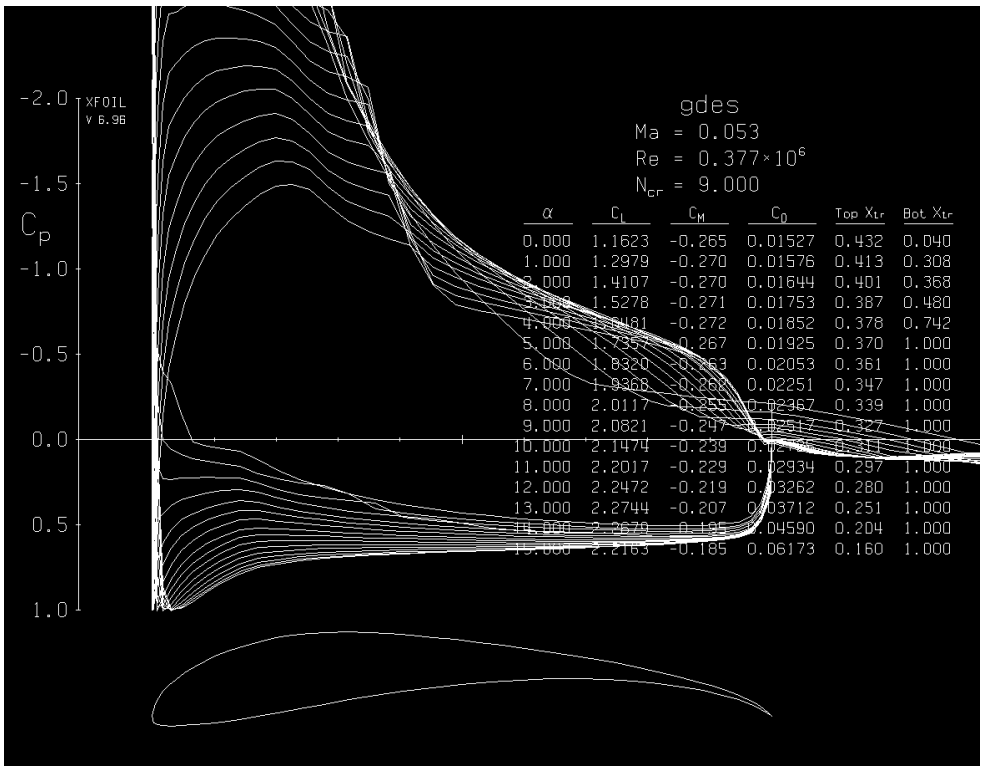

Figure 4: Sweep of angle of attack for airfoil performance (S1223)

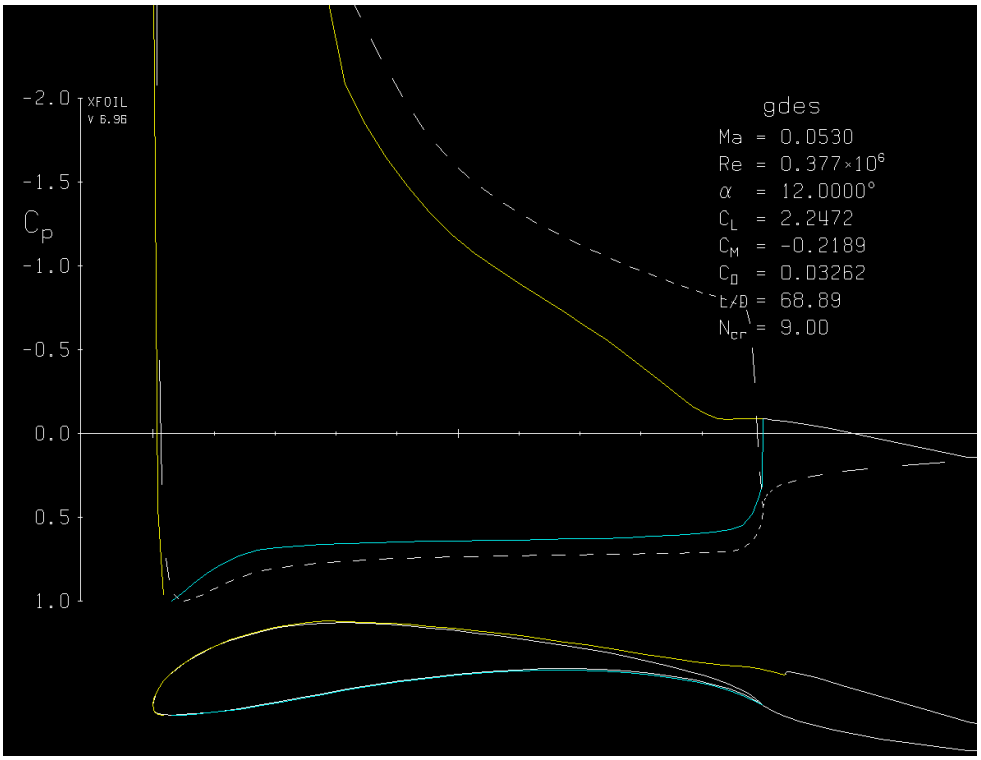

Figure 5: Airfoil (S1223) performance for 12° angle of attack

Following XFOIL analysis, a comprehensive table of wing geometry and performance characteristics was generated with the use of the team's MATLAB code. The result can be seen below in **Figure 6**. These results provide an acceptable shape for the first iteration. The geometry is reasonable, the lift provided is adequate, and the drag is acceptable.

Summary of Wing Geometry

Chord at Root [ft]	Taper Ratio	Chord at Tip [ft]	Wingspan [ft]	Wing Planform [ft^2]	Aspect Ratio
1.0	0.5	0.50	8.8	6.6	11.73

Performance Characteristics

cl	cd	delta	AoA	Flight Speed [m/s]	Reynolds number	CL	cD induced	cD 3D	CD	Lift [lbs]	Drag [lbs]
2.247	0.033	0.03	12.0	17.88	3.77e+05	2.247	0.142	0.143	0.284	60.00	7.59

Figure 6: Performance characteristics and wing geometry

Subsequent iterations of this process will attempt to improve upon this basis by fine-tuning the flight speed once that information is understood, adjusting the airfoil to perform more efficiently in known operating conditions, and finally carrying out wind tunnel tests to validate these results.

4. Propulsion Analysis

One of the first key steps in propulsion analysis was the selection of the motor. Our group has selected the Magnum XLS .61A motor due to the ease of access over the other motor option. No modifications to motor or exhaust are allowed for this competition. The key properties for this motor can be seen in the **Table 1** below.

Table 1: Magnum XLS-61A specifications

Magnum XLS-61A	
Displacement	9.94cc (0.607ci)
Bore	24mm
Stroke	22mm
Practical RPM	2,000 – 16,000 rpm

For the analysis of the motor, the engine displacement of .607 cubic inches and the practical rpm range of 2,000-16,000 rpm must be taken into consideration. The Top Flite propeller manufacturing company has developed the figure below. The figure plots engine displacement along the bottom axis and a curve across the plot defines the practical rpm range for the given engine displacement. From the start and endpoints of the practical rpm, the range of the propellers can be defined.

5. Material Selection

With strength to weight optimization being vital for aircraft design, this team has chosen to utilize rapid prototyping technology to construct wing ribs. This allows the airfoil to be modeled with high precision, vital to both the aerodynamics and accurate analysis of a wing. By utilizing this technology, ribs may be produced that are both significantly stronger and more exactly manufactured than if they were to be constructed of a typical model aircraft material such as balsa or bass wood.

The rapid prototyping technology available to us uses a polymer known as Acrylonitrile Butadiene Styrene P400 (ABS). **Table 2** shows some of the main characteristics of ABS P400.

Table 2: ABS Properties

Specific Gravity	Tensile Strength (Mpa)	Tensile Modulus (Mpa)	Flexural Strength (Mpa)	Flexural Modulus (Mpa)
1.04	22	1,627	41	1,834

As seen above, ABS has a specific gravity of 1.04, almost five times that of balsa wood. Conversely, this polymer has high potential for impact and mechanical strengths.

Due to ABS's woven construction, these strengths extend in all planar directions, which is a significant advantage when compared to an equivalent fibrous rib (wood), whose strength is related to an applied force's orientation to the grain.

6. Spar Analysis

Modeling of the spars depends on the load distribution along the wing. This load will be provided through the aerodynamics portion of the calculations. Analysis of each spar will be communicated via a discretization of the planar-area of the wing, and the corresponding static and material analysis.

6.1. Wing Discretization

The wing will consist of two main supports, a front spar and rear spar. To ultimately determine the stresses acting along each, the wing must first be broken into sub elements, marking the space between wing ribs. Arranged from A_1 to A_n, this breakdown is given in **Figure 7** located on the ensuing page.

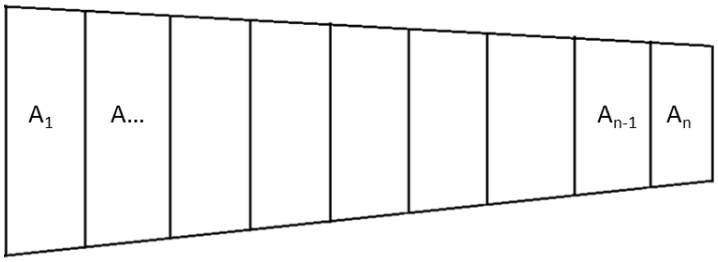

Figure 7: Discretization of Wing

Each sub element can be best modeled as a trapezoid because of the linearly tapered airfoil planform. Generalized dimensions are outlined in **Figure 8** below, and calculated explicitly in Appendix B.

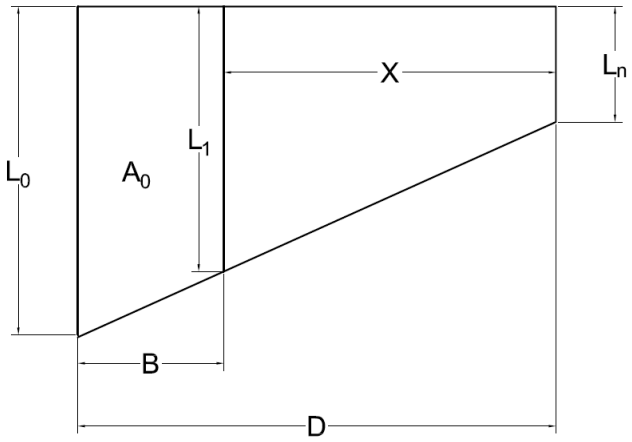

Figure 8: Wing Dimensions

This process of discretization enables the engineer to determine the percent area of the total wing area exists between individual ribs. By applying the percent planform area as a multiplied scalar to the total lift force per wing, the lift force acting over each section can be determined, as in Appendix B, Equation 1-A.

6.2. Representative Model/ Static Analysis

Knowing the load trends across the wing, shear force and bending moment diagrams may be constructed to determine locations where analysis should be focused towards. To build these diagrams, lift forces are considered to be acting at the same location as the center of gravity of each wing element, given in Appendix B, Equation 2.

With these diagrams constructed as seen in Appendix B, the engineer may interpolate to determine maximum forces acting along the wing; in the case of a cantilevered beam, mechanical failure is most likely to occur at the fixed end.

6.3. Mechanics of Materials

With shear and bending forces tabulated across the length of the wing, material analysis becomes a balancing between consideration of the torques induced about each rib, and the analysis of the spar along its length of the wing

6.3.1. Torque about ribs

Based on angle of attack and the lift force profile determined from airfoil analysis, the percent of the lift forces acting on the front and rear spars may be taken as 70% and 30%, respectively. These connected spars are related by a moment couple about the elastic center of the rib, given in Appendix B, Equation 3. This equivalent force corresponds to a torsional displacement given in Appendix B, Equation 4.

One important implication of this relation is that in-flight torque on the wings may be practically negligible if the elastic center is designed to be at the point at which the lift force resolves.

6.3.2. Spars along length of wing

With the loading of the wing known, materials and stress analysis may be performed at the fixed end, indicating the maximum stresses that the airfoil will experience.

7. References

[1] Raymer, Aircraft Design: A Conceptual Approach

[2] Johnson, Airfield Models, http://airfieldmodels.com/

[3] Anderson, Fundamentals of Aerodynamics

[4] https://store.amtekcompany.com/products.php?product=Dimension-Standard-ABS-Model-Material-%25252d-P400

[4] http://www.rc-airplane-world.com/propeller-size.html

[5] Magnum XLS .61a Operating Instructions, http://media.globalhobby.com/manual/210770.PDF

[6] XFOIL, raphael.mit.edu/xfoil/

8. Appendices

8.1. Appendix A

```
%%%%%%%%%%%%%%%%%%%%%%%%%%%%%%%%%%%%%%%%%%%%%%%%%%%%%
%%%%%%%%%%%%%%%%%%%%%%%%%
%   Program: Nelessen_AeroDesign.m
%   Programmer: Adam Nelessen
%   Institution: Northern Arizona University
%   Date: Fall 2012
%   Performed for: SAE Aero Design West Airplane
%%%%%%%%%%%%%%%%%%%%%%%%%%%%%%%%%%%%%%%%%%%%%%%%%%%%%
%%%%%%%%%%%%%%%%%%%%%%%%%
%% Cleanup
clear all; clc; close all;

%% Input Environmental Variables
speed_mph=30:.1:50;                  %[mph]Predicted speeds from previous team's report
speed_mps=speed_mph.*.4470;          %[m/s]
speed_particular=40*.447;            %[m/s]
alpha=12;                            %degrees
T=283.15;                            %[K] from wunderground avg on 4/14
p=98532.6;                           %[Pa] from wunderground avg on 4/14
R=287.04;                            %[J/kg*K] Air
rho=p/(R*T);                         %[kg/m^3]
mu=1.71E-5*(T/273)^0.7;              %[N*s/m^2] From Power Law eqn., Table A.2, pg. 826, Fluid
Mechanics by White

a=337.4;                             %[m/s] at T=283K
Mach=speed_mps./a;
Mach_particular=speed_particular/a;

qinf=.5*rho.*speed_mps.^2;
qinf_particular=.5*rho*speed_particular^2;

%%
%%%%%%%%%%%%%%%%%%%%%%%%%%%%%%%%%%%%%%%%%%%%%%%%%%%%%
%%%%%%%%%%%%%%%%%%%%%%%
%%%%%%%%%%%%%%%%Determine wing planform from airfoil
analysis%%%%%%%%%%%%%%
%%%%%%%%%%%%%%%%%%%%%%%%%%%%%%%%%%%%%%%%%%%%%%%%%%%%%
%%%%%%%%%%%%%%%%%%%%%%%%%
chordft=1;%input('\nInput Chord at the root in ft: \n');
chord=chordft*.3048;
cl=2.2472;%input('\nInput cl from XFOIL: \n');
Lprime=cl*qinf_particular*chord;
taper=.5;%input('\nInput wing taper ratio:\n');
if taper ==0
   ctip=chord;
```

```
else
    ctip=taper*chord;
end
ctipft=ctip/.3048;
Lsquare=80*4.448;


b=Lsquare/Lprime;
bft=b/.3048;
Lfraction=1-(b*(chord-ctip))/(2*b*chord);
Ltapered=Lfraction*Lsquare;
Ltaperedlbs=Ltapered/4.448;


S=b*ctip+(chord-ctip)*(b/2);
Sft=S/(.3048^2);
AR=b^2/S;

CL=Ltapered/(qinf_particular*S);
delta=-3.3333*taper^6 + 10.481*taper^5 - 10.638*taper^4 + 2.4984*taper^3 + 2.2357*taper^2 -
1.2996*taper^1 + 0.2007;
cDinduced=(CL^2*(1+delta))/(pi*AR);
cd_xfoil=0.03262;
cD_3D=cd_xfoil*b/S;
CDtotal=cDinduced+cD_3D;
D=CDtotal*qinf_particular*S;
Dlbs=D/4.448;

%%
%%%%%%%%%%%%%%%%%%%%%%%%%%%%%%%%%%%%%%%%%%%%%%%%%%%%%%%%%%%%
%%%%%%%%%%%%%%%%%%%%%%%%
%%%%%%%%%%%%%%%%%%%%Calculate Reynolds
Number%%%%%%%%%%%%%%%%%%%%%%%%%%%%%%%%%%%%%%%%%%%%%%%%%%%%%%%%%%%%%%%%%%%%%%%%%%%%%
%%%%%%%%%%%%%%%%%%%%%%%%%%%%
chordRe=chord*.3048;                        %[m]
Re=(rho.*speed_mps.*chord)./mu;         %Theoretical Range
Re_particular=(rho*speed_particular*chord)./mu;

%%
%%%%%%%%%%%%%%%%%%%%%%%%%%%%%%%%%%%%%%%%%%%%%%%%%%%%%%%%%%%%
%%%%%%%%%%%%%%%%%%%%%%%%
%%%%%%%%%%%%%%%%%%%%Output Significant
Results%%%%%%%%%%%%%%%%%%%%%%%%%%%%%%%%%%%%%%%%%%%%%%%%%%%%%%%%%%%%%%%%%%%%%%%%%%%%%
%%%%%%%%%%%%%%%%%%%%%%%%%%%%
fprintf('                                        Summary of Wing Geometry                              \n');
fprintf('\n');
fprintf('       | Chord at Root  |  Taper Ratio  |  Chord at Tip   |  Wingspan  |  Wing Planform  | Aspect
Ratio  |\n');
fprintf('       |-------[ft]------|---------------|-------[ft]-------|----[ft]----|-----[ft^2]------|---------------|\n');
```

```
fprintf('      |      %.1f      |      %.1f      |      %.2f      |      %.1f      |      %.1f      |      %.2f      | \n',chordft,
taper,ctipft, bft, Sft,AR);
fprintf('\n');
fprintf('\n');
fprintf('                                    Performance Characteristics                                    \n');
fprintf('\n');
fprintf('|  cl   |  cd   | delta | AoA  | Flight Speed | Reynolds number | CL  | cD induced | cD 3D |   CD   |
Lift   |  Drag   |\n');
fprintf('|-------|-------|-------|------|----[m/s]-----|-----------------|-----|------------|-------|-------|--[lbs]--|--[lbs]--
|\n');
fprintf('| %.3f | %.3f | %.2f  | %.1f |    %.2f     |    %1.2e     |%.3f|   %.3f    | %.3f | %.3f |  %.2f  |   %.2f  |\n',
cl, cd_xfoil,delta, alpha, speed_particular,
Re_particular,CL,cDinduced,cD_3D,CDtotal,Ltaperedlbs,Dlbs);
```

8.2. Appendix B

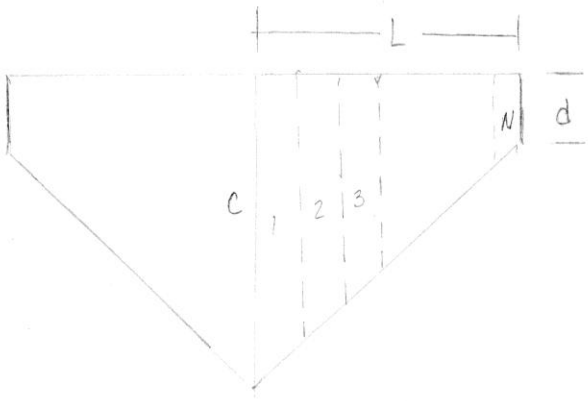

- $L = \frac{\text{WING SPAN}}{2}$
- C = CHORD
- $F_{LIFT} = \frac{F_{LIFT\ TOTAL}}{2}$
- α = ANGLE

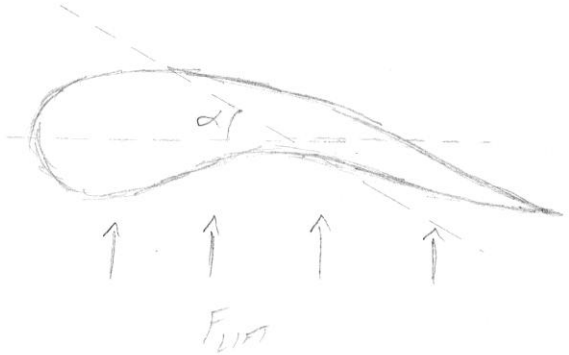

LIFT PER SECTION

AREA FOR EACH SUBELEMENTS

FOR $i = 1:N$

(1) SECTION AREA (%) $(A_{SEC}) = \frac{\left[\frac{d_{i-1} + d_i}{2}\left(L/N\right)\right]}{\left[\frac{c+d}{2}\left(L\right)\right]}$

WHERE

$$d_i = \left(\frac{L\,i}{N}\right)\left(\frac{c-d}{L}\right)$$

(1-A) $\Rightarrow F_{LIFT,\,SECTION} = (A_{SEC})(F_{LIFT})$

CENTER OF GRAVITY

(2) $CG(x) = \frac{d_{i-1} + d_i}{3(d_{i-1} + d_i)} + L\left(\frac{i-1}{N}\right)$

- $F_{LIFT,\,SECTION}$ ACTS AT $CG_{SECTION}$

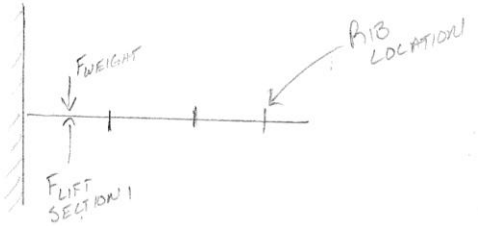

V & M DIAGRAMS

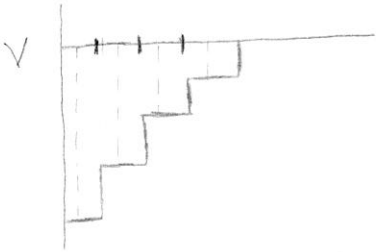

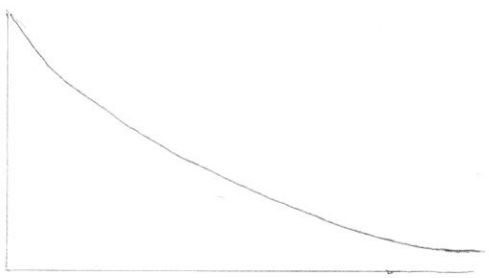

INTERPOLATE TO DETERMINE V & M AT ANY POINT.

TORQUE

ELASTIC CENTER.

(3) $E(x) = \frac{a_0}{b_0} = \frac{E_{FS} I_{FS}}{E_{RS} I_{RS}}$

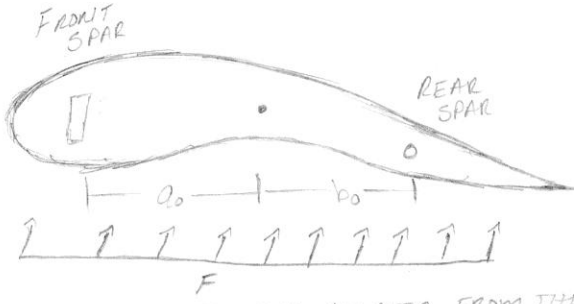

TORQUE DETERMINED BY HOW FAR THE RESOLVED FORCE IS LOCATED FROM THE ELASTIC CENTER.

(4) $\theta = \frac{F L''}{8 b A_0}$

WHERE

$\frac{1}{A_0} = \frac{1}{A_F} + \frac{1}{A_R}$

- $A_F = E I_F$
- $A_R = E I_R$

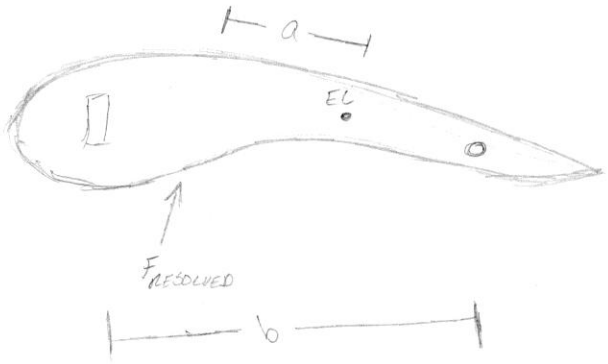

MECHANICS OF MATERIALS

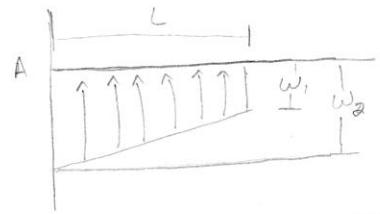

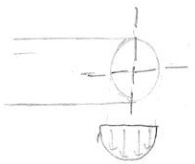

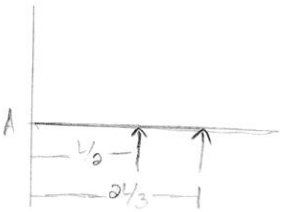

$\Sigma M_A = \frac{L}{2}(\omega_1 L) + \frac{2L}{3}[(\omega$

$\sigma = \frac{M y}{I}$ (5)

σ IS MAX WHEN "y" ON THE TOP & BOTTOM THE SPAR